Asian Journal of Chemistry; Vol. 25, No. 4 (2013), 2308-2314

ASIAN JOURNAL OF CHEMISTRY

http://dx.doi.org/10.14233/ajchem.2013.14280

Synthesis and Density Functional Theory Studies of *Octakis*(propyl) Porphyrazine and Its Fe(II) Complex

MILLICENT K. MONGALE, DAVID A ISABIRYE, MWADHAM M. KABANDA and ENO E. EBENSO*

Department of Chemistry, School of Mathematical and Physical Sciences, North-West University (Mafikeng Campus), Private Bag X2046, Mmabatho 2735, South Africa

*Corresponding author: E-mail: Eno.Ebenso@nwu.ac.za

(*Received*: 13 July 2012; *Accepted*: 25 October 2012) AJC-12337

The synthesis and characterization of metallated porphyrazine compounds is gaining increasing attention because of the numerous functionalities for this class of compounds. In this study synthesis and quantum chemical calculations (utilizing the B3LYP/6-31G(d,p) method) on 2,3,7,8,12,13,17,18-octakis(propyl)porphyrazine ligand and its iron metallated complex have been investigated to determine the metallation effects on the electronic and geometric properties of the ligand. The time-dependent density functional theory (TDDFT) approach was utilized for the analysis of the UV-visible spectra. The variation in geometric parameters, HOMO-LUMO gap, dipole moment and Mulliken atomic charges suggest that metallation induces significant geometric changes that is dependent on the spin state of iron. A comparison of porphyrazine ligand and 2,3,7,8,12,13,17,18-octakis(propyl)porphyrazine ligand suggests that alkylation has minimal influence on the geometry of the porphyrazine moiety.

Key Words: Porphyrazine synthesis, DFT studies, HOMO-LUMO gap.

INTRODUCTION

Porphyrazine (Pz) derivatives have wide applicability in areas such as liquid crystals formation, electrocatalysis, photodynamic therapy, gas sensors and as optical data storage[1-11]. Various applications of porphyrazine derivatives could be attributed to the several properties of its molecules which can be modified to suit the task specificity. Because of their wide applicability and potential uses, there is an increase in the search for porphyrazine derivatives with potential biological and technological uses. For instance, the importance of iron porphyrazine derivatives are notably reported in biological systems and biomimetic catalytic reactions and have lead to increased studies on the synthesis of iron porphyrazine compounds[12-14]. While experimental methods are utilized in the synthesis procedure, there is an increase in the application of quantum chemical methods to elucidate the molecular properties of porphyrazine derivatives and explain the effects of metallation and other substituent effects on the porphyrazine moiety[15-18].

The objective of this work is to report the results of the synthesis of 2,3,7,8,12,13,17,18-*octakis*(propyl)porphyrazine ligand (abbreviated in this work as oct(pr)Pz) and 2,3,7,8,12,13,17,18-*octakis*(propyl)PzFe(II) compound (abbreviated in this work as oct(pr)PzFe(II)) and to study the effects of metallation on the molecular properties of the metal free *octakis*(propyl)porphyrazine. Moreover, density functional theory calculations were also done for the porphyrazine base to investigate the effects of alkylation of the porphyrazine base. To achieve this, ground-state geometric parameters (*e.g.*, bond lengths and bond angles) and electronic properties (*e.g.*, net atomic charges, HOMO and LUMO energies and dipole moment) of the studied compounds are analyzed and compared across structures. The schematic representations of the studies compounds are shown in Fig. 1. To our knowledge, there is no literature work on oct(pr)Pz ligand and oct(pr)PzFe(II), which makes the synthesis and the characterization of these compounds an interesting work.

EXPERIMENTAL

All the reagents used were obtained from UnivAR, Saarchem and Merck Chemical (Pvt.) Ltd. Solvents used for reactions were distilled prior to use: dichloromethane (from CaH_2); dimethylformamide (pre-dried from barium oxide) distilled in alumina; Tetrahydrofuran (THF) was heated over sodium benzophenone under nitrogen (N_2) until a blue colour persisted with subsequent distillation under nitrogen prior to use; butanol and methanol (in magnesium).

Thin-layer chromatography (TLC) was carried out on E. Merk 60 F_{254} silica gel plates. Flash chromatography was on E. Merck silica gel 60, 40-60 μm. Infra-red spectra were recorded on a nicolet 410 impact fourier transform infrared

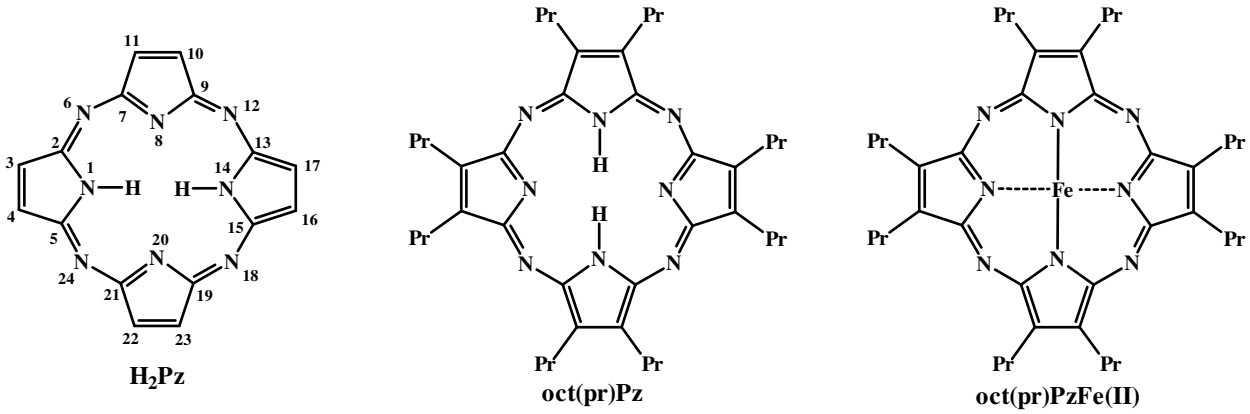

Fig. 1. Schematic representations of the studied compounds. The atom numbering necessary for discussion are shown in the H_2Pz structure

spectrophotometer using nujol and potassium bromide cells. The range of interest was between 4000 and 500 cm^{-1}. The ultraviolet-visible absorption spectra were measured in a 1-cm quartz cell using either a Unicam SP 8700 spectrophotometer or a Varian Cary 50 ultraviolet-visible spectrophotometer. Measurements were made from 300 nm to 700 nm. The ^1H and ^{13}C NMR spectra of the compounds were recorded on a Varian-Gemini-300 (300 MHz) spectrometer in $CDCl_3$. ^1H NMR data (300 MHz) are listed in order of chemical shift (δ) reported in ppm and referenced to the residual solvent peak of $CDCl_3$ (7.24 ppm). The coupling constant *J* (Hertz) is reported to the nearest 0.1 Hz and multiplicities are given as follows: s (singlet), d (doublet), t (triplet), dd (doublet of doublet), q (quartet), hp (heptet) and m (multiplet). Proton decoupling experiments were performed to help out in the assignment of proton signals. ^{13}C NMR data are listed in the order: chemical shift (δ) in ppm and referenced to the residual solvent peak of $CDCl_3$ (δ = 77.0 ppm).

Synthesis of compounds

4,5-Dibromo-4E-octene precursor: Bromine solution (15.05 mL, 0.186 mol) in acetic acid (250 mL) was added drop-wise to 4-octyne (80 mL, 0.180 mol), which was dissolved in acetic acid (80 mL). The addition was performed at such a rate that there was no orange colour formed. When the addition was complete, the solution was stirred for an additional 0.5 h and then poured into ice water (800 mL). This was followed by extraction with dichloromethane (300 mL × 4). The dichloromethane extract was washed with a solution of sodium hydrogen carbonate (300 mL × 3) followed by water (300 mL × 3). The extract was then dried over anhydrous magnesium sulphate and filtered. The solvent was removed by rotary evaporation to yield a yellow crude oil (56 g, 52 %).

2,3-Dipropylfumaronitrile precursor: Copper(I) cyanide (24.49 g, 0.277 mol) in dimethylformamide (250 mL) was heated to 145 ºC until the solution became clear which was then allowed to cool down to 130 ºC. This was followed by an addition of 4,5-dibromo-4E-octene (23.120 g, 0.088 mol). The reaction was heated for 15 h at 130 ºC. Thereafter, the solution was allowed to cool to room temperature and then it was carefully poured into concentrated ammonium hydroxide (600 mL). After stirring for 40 min, the blue suspension was filtered and the residue was washed with ethyl acetate until ethyl acetate became colourless. The filtrate was extracted with ethyl acetate (200 mL × 3). The ethyl acetate extract and washings from the solids were washed with water (200 mL × 3), followed by sodium chloride (200 mL × 2). The organic layer was dried with anhydrous magnesium sulphate. The resulting brown oil was purified by vacuum distillation to give clear oil (5.1 g, 39 %).

2,3-Dipropylmaleonitrile precursor: 2,3-Dipropylfumaronitrile (6.335 g, 0.043 mol) in acetonitrile (150 mL) was dissolved in a Rayonet photochemical reactor round bottom flask that was sealed with a septum. Nitrogen was bubbled through the solution, during stirring. The solution was irradiated with light of wavelength 253 nm for 72 h. During the irradiation, the temperature of the reaction mixture rose by about 40 ºC owing to the heat given by off by the reactor lamps. When a period of 72 h had elapsed, the reaction reached a photostationary state and was stopped. The solvent was removed by rotary evaporation and the *cis* and *trans*-isomers were separated by fractional distillation under high vacuum. The *trans*-isomer was distilled at about 40 ºC, a lower temperature than that for the desired *cis*-isomer which was obtained as a clear oil. The yield was 2.0 g, 32 %).

Synthesis of oct(pr)PzMg(II): A suspension of magnesium (75 mg, 3.09 mmol) and iodine crystals (2.56 g, 0.01 mol) in dry butanol (25 mL) was heated under reflux under nitrogen. The resulting solution was cooled down to room temperature followed by addition of 2,3-dipropylmaleonitrile (300 mg, 0.831 mol) and the reaction mixture again refluxed for 24 h in darkness. The brownish purple solution was obtained. The solvent then evaporated under low pressure. The crude product was chromatographed (hexane/ethyl acetate, 8:1) to give a pure sample of *octakis*(propyl)PzMg(II) complex (0.2 g, 38 %).

Incorporation of Fe (II) cation into the *octakis*(propyl)-Pz base: Ferrous sulphate (2.780 g, 1 mmol) was dissolved in dimethylformamide to make a concentration 0.1 M in a 100-mL volumetric flask. Then the solution of iron(II) was mixed with the free base ligand (5×10^{-5} M in dimethylformamide) until a uniform solution was attained. This mixture was heated for 1 h to ensure complete reaction of the iron(II) under a nitrogen-controlled environment. Subsequently, the solvent was removed by rotary evaporator at a controlled temperature of 110 ºC. A dark green residue was collected and washed with chloroform (250-mL). The solvent was removed by rotary evaporator giving dark green oil (2.1 g, 32 %).

Computational details: The optimized geometries were obtained utilizing density functional theory (DFT) method with the B3LYP functional. The 6-31G(d) basis set was selected for all the calculations as a compromise between computational affordability and results meaningfulness. The B3LYP/6-31G(d) method has been found to provide adequate description of the geometry and other molecular properties of different macrocycle molecules[19,20]. The vertical excitation energies were calculated by means of the time-dependent density functional theory (TDDFT) method. Time-dependent density functional theory has been successful applied in the prediction of the electronic absorption spectra of a number of different macrocycles[21-25].

Frequency calculations were performed on optimized geometries to establish the nature of the stationary point on the potential energy surface. The geometry optimizations were performed by using the Spartan program[26] while the UV-VIS spectra were performed by using the Gaussian program[27].

RESULTS AND DISCUSSION

Synthesis of *octakis*(propyl)PzMg(II) complex: *Octakis*(propyl)PzMg(II) complex was successfully prepared *via* Linstead's magnesium template *tetra*-macrocyclization reaction of maleonitrile or fumaronitriles[28]. Maleonitrile and fumaronitriles were synthesized by the Rosenmund-von Braun reactions and *trans*-dibromoalkenes were used as substrates[29-31]. In the presence of acetic acid, dibromooctene was prepared by reacting octyne with bromine. This resulted in the formation of 4,5-dibromo-4E-octene as an electrophilic reaction occurred where bromine was added to the triple bond of the octyne. The vinylic dibromides were then converted to fumaronitriles. Fumaronitriles (*cis*-isomer) were converted into maleonitriles (*trans*-isomer) by UV irradiation sourced by mercury lamp for 30 h. As the reaction proceeded, photostationary state was reached consisting of approximately equal amounts of *cis*- and *trans*-dinitriles. Separating the two proved difficult due to their close R_f values. However, when vacuum distillation was utilized, the required maleonitrile was obtained as clear oil at a yield of about 30 %. The ^{1}H NMR and ^{13}C NMR of fumaronitrile and maleonitrile closely resemble one another due to the fact that the two are isomeric. The yield of oct(pr)PzMg(II) complex was observed to be lower when starting material was fumaronitrile than when starting material was maleonitrile. To ensure effective cyclization, the two nitrile groups had to be on the same side of the ring and their reaction resulted in a number of different porphyrazines which were separated by column chromatography.

Synthesis of *octakis*(propyl)Pz base and the incorporation of Fe(II) cation: Demetallation of oct(pr)PzMg(II) was achieved by heating at reflux the magnesium porphyrazine in a $CHCl_3/CH_3COOH$ (20:1) solution (**Scheme-I**). The solvent was then slowly removed by rotary evaporation in order to avoid aggregation of the products mixture. The reaction was performed under nitrogen so as to avoid the formation of the *seco*-porphyrazine due to the opening of one of the pyrrole rings. This was found to be problematic during the metallation of the complex because instead of central metallation peripheral metallation will take place in the case of a *seco*-porphyrazine. The Fe (II) cation metallation of *octakis*(propyl) Pz free base was achieved by heating a solution of ferrous sulphate and the ligand in dimethylformamide for 1 h (**Scheme-I**).

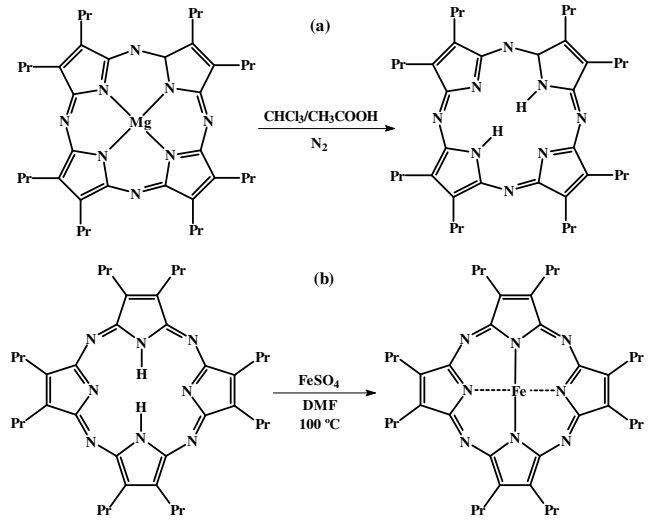

Scheme-I: Synthesis of *octakis*(propyl)PcFe(II) initiated by (a) demetallation of *octakis*(propyl)PcMg(II) and propagated by (b) metallation of *octakis*(propyl) base with Fe(II)

The ^{1}H NMR spectrum of the free-base (*i.e.*, after the removal of the magnesium ion) showed splitting at high field, 2.11 ppm which was due to the two protons, one on N1 and the other on N14. The methyl groups of the propyl substituents were also observed at high field of 1.86 ppm and were reflected as triplet. A quartet was observed at 3.98 ppm and it was due to protons attached to carbons which were linked directly to the pyrrolic rings. All these assignments are consistent with published data[28,32-34] and confirm the structure of synthesized compound.

Ultraviolet visible spectrum of meta free and the metallated oct(pr)Pz base: The UV-VIS spectra of the free-base and the Fe(II) metallated porphyrazine are shown in Fig. 2 respectively. The figure shows a Soret band at 340 nm (1.363 abs) and 558.0 nm (0.783 abs) and a split Q-Bands at 626.1 nm (Q_y, 1.244 abs) and at 598.0 nm (Q_y, 0.234 abs). Moreover, the results also indicate that metallation reduces the symmetry of the ligand from D_{4h} to D_{2h} in which two lowest energy unoccupied orbitals are no longer degenerate[35]. Gouterman's[36] four orbital model provides a qualitative description of the reductive effect the metal removal have on the symmetry of the complex. According to this theory, the absorption bands in porphyrazine systems arise from transitions between two HOMOs (a_{1u}, a_{2u}) and two LUMO (e_g).

The electronic spectra of the of iron(II) insertion into the oct(pr)Pz ligand showed the change at 598 nm, which confirms the insertion of iron(III) cation into the free-base. The other peaks were blue shifted, a Soret peak at -7.00 nm and the Q band at -1.1 nm.

Proposed mechanism for iron(II) incorporation: The incorporation of Fe(II) metal ion into the oct(pr)Pz ligand can occur in two ways. The first mechanism would be the removal of the central magnesium(II) metal ion from the macrocycle, followed by a fast pick up of the Fe(II) metal ion by the resulting free base;

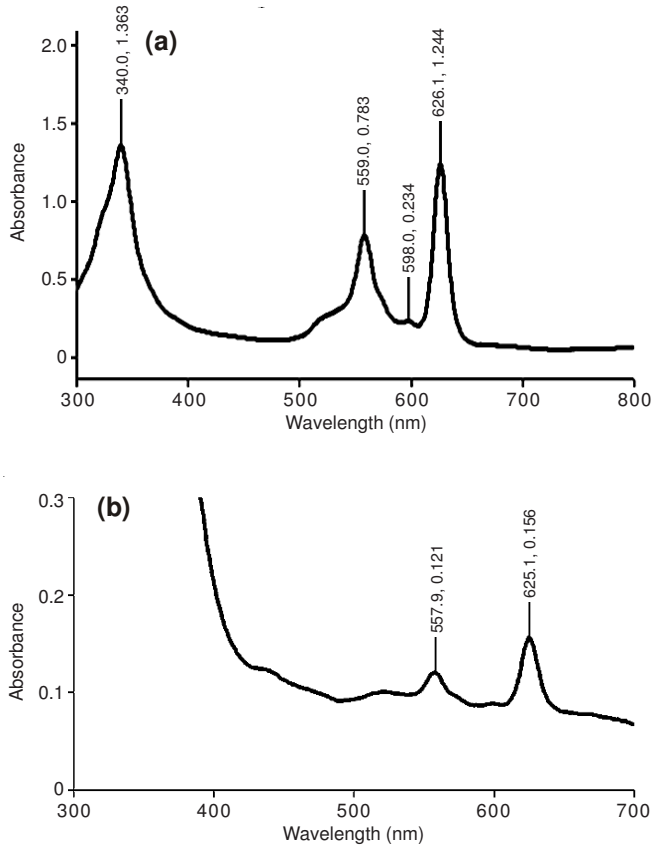

Fig. 4. UV-visible spectra of (a) *octakis*(propyl)Pz and (b) *octakis*(propyl)-PzFe(II). UV-visible was determined in dimethylformamide solution

$$[Pz]Mg \xrightarrow[\text{fast}]{\text{acetic acid}} [Pz] + Mg^{2+} \quad (2)$$

$$[Pz] + Fe^{2+} \xrightarrow[\text{slow}]{} [Pz]Fe \quad (3)$$

The second mechanism involves a direct exchange of positions between the iron(II) metal ion and the Mg(II) metal ion without forming the free base;

$$[Pz]Mg \xrightarrow{Fe^{2+}} [Pz]Fe \quad (4)$$

Since the rate constant for the direct incorporation of Fe^{2+} into the oct(pr)Pz free base is similar to that of incorporation into the oct(pr)PzMg(II), it is reasonable to infer that the reaction follows the first route.

Redox reaction: The reaction conditions utilized for the oxidation of oct(pr)PzFe(II) complex with oct(pr)PzCr(III) complex are such that the position of the isosbestic points was 611.9 nm, the reaction was followed at the wavelength of 374.8 nm and the activation energy for the reaction was 1.02 (unit). The absorbance *versus* time plot for the oxidation reaction, suggests that the rate of oxidation of iron(II) to iron (III), increases with the increase in temperature. The activation energy of 32.7 kJ mol^{-1}, for the Fe(II) insertion reaction, was estimated from the plot of ln k *vs* 1/T and by using the principles of the Arrhenius equation. The proposed mechanism of the oxidation of oct(pr)PzFe(II) by oct(pr)PzCr(III) is an outer-sphere reaction mechanism. This is because the porphyrazine to which the Fe(II) metal ion is coordinated does not have a bridging group, which is common to the coordination sphere of both oct(pr)PzFe(II) and oct(pr)PzCr(II). The oxidation reaction therefore followed an electron tunneling mechanism. Although such reactions are fast, the size of the macro cycle clearly affected the rate. For the reaction to take place the reactants have to rearrange before electron transfer could take place to satisfy the Franck Condon requirements which stipulates that the oxidant and the reductant must reorganize themselves before the act of electron transfer in a way that ensures the energies of the oxidant and reductant in their transition state are identical.

Quantum chemical studies

Geometric and electronic parameters: The optimized geometries of the non-alkylated free Pz, free oct(pr)Pz and the oct(pr)PzFe(II) shown in Fig. 3. The non-alkylated free porphyrazine was included in the study to investigated the influence of the alkyl chains on the properties of the porphyrazine molecule. All three spin states of Fe(II) (*i.e.*, s = 0, s = 1 and s = 2) were considered and the optimized structures are shown in Fig. 3. The geometric parameters (*i.e.*, bond lengths and bond angles) for all the structures are shown in Table-1. A comparison of the bond lengths and bond angles for non-alkylated free porphyrazine and free oct(pr)Pz suggests that alkylation has no significant influence on the properties of the free porphyrazine base. However, a comparison of the bond lengths and bond angles for free oct(pr)Pz and the oct(pr)PzFe(II) with Fe(II) in three spin states, suggests that metallation has significant influence on the geometry of the porphyrazine and that the geometric effects depends on the spin state of Fe(II) considered. The change in the bond lengths upon metallation is an indication of the changes in the electron cloud of the corresponding bonds which is a result of the change in the molecular symmetry. For instance, an increase in the bond length suggests that there is a decrease in the electron cloud of the bond type considered and a decrease in the bond length suggests that there is an increase in the electron cloud of the bond type considered.

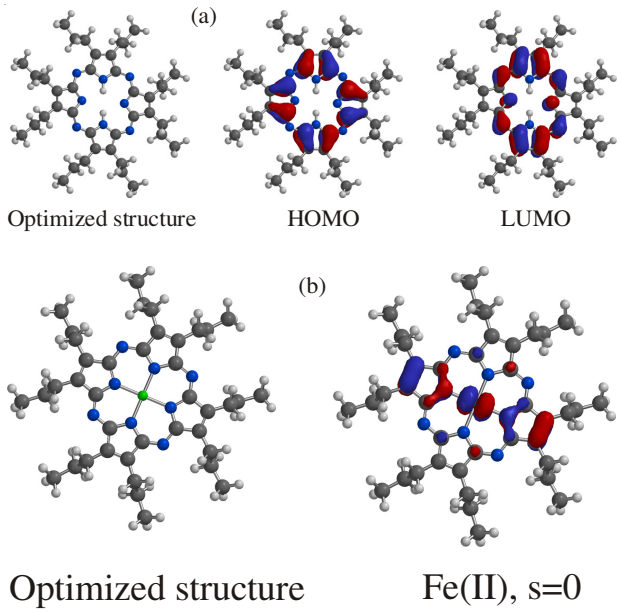

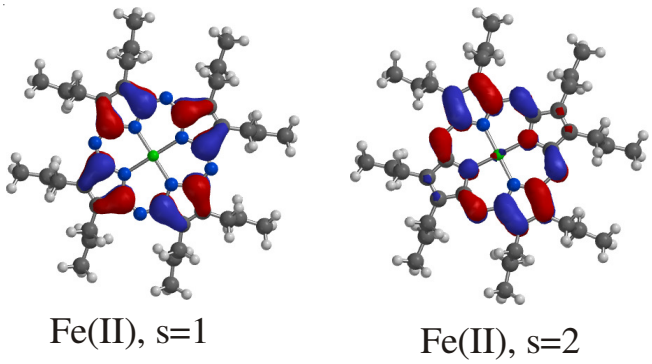

Fig. 3. Optimized structure and the highest occupied molecular orbital for (a) oct(pr)Pz metal free and (b) oct(pr)PzFe(II) with Fe(II) in spin states of s = 0, s = 1 and s = 2

TABLE-1
SELECTED BOND LENGTHS (Å) AND BOND ANGLES (°) FOR THE PORPHYRAZINE DERIVATIVES IN THE METAL FREE AND IN THE COMPLEXED FORM

Geometric parameters	H_2Pz	oct(pr) Pz	oct(pr)Pz Fe(II) Fe(s=0)	oct(pr)Pz Fe(II) Fe(s=1)	oct(pr)Pz Fe(II) Fe(s=2)
BOND LENGTH					
N1-C2	1.372	1.372	1.384	1.373	1.394
N1-C5	1.371	1.371	1.383	1.374	1.394
C2-C3	1.454	1.454	1.443	1.459	1.458
C3-C4	1.378	1.378	1.381	1.370	1.367
C4-C5	1.453	1.454	1.443	1.459	1.458
C2-N6	1.324	1.323	1.330	1.328	1.307
N6-C7	1.338	1.338	1.322	1.329	1.347
C7-N8	1.361	1.362	1.376	1.374	1.392
N8-C9	1.362	1.362	1.376	1.373	1.392
C7-C11	1.475	1.476	1.467	1.459	1.421
C9-C10	1.475	1.475	1.467	1.459	1.421
C10-C11	1.363	1.363	1.362	1.370	1.397
C9-N12	1.338	1.338	1.322	1.328	1.346
N12-C13	1.323	1.323	1.330	1.328	1.307
C13-N14	1.371	1.372	1.384	1.373	1.394
N14-C15	1.372	1.371	1.383	1.374	1.394
C13-C17	1.453	1.454	1.443	1.459	1.458
C15-C16	1.454	1.454	1.443	1.459	1.458
C16- C17	1.378	1.378	1.381	1.370	1.367
C15-N18	1.324	1.323	1.330	1.329	1.307
N18-C19	1.338	1.338	1.322	1.329	1.346
C19-N20	1.361	1.361	1.376	1.373	1.392
N20-C21	1.362	1.362	1.376	1.373	1.393
C19-N23	1.476	1.476	1.467	1.459	1.421
C21-C22	1.476	1.476	1.467	1.459	1.421
C22-C23	1.363	1.363	1.362	1.371	1.397
C21-N24	1.338	1.338	1.330	1.329	1.347
N24-C5	1.323	1.323	1.322	1.329	1.307
BOND ANGLE					
C2N1C5	110.5	110.5	105.8	106.3	106.0
C2N6C7	123.1	123.1	121.9	122.3	121.5
C7N8C9	105.0	105.0	105.5	106.2	105.5
C9N12C13	123.1	123.1	121.9	122.2	121.5
C13N14C15	110.5	110.5	105.8	106.3	106.0
C15N18C19	123.1	123.1	121.9	122.3	121.5
C19N20C21	105.0	105.0	105.5	106.3	105.5
C21N24C5	123.1	123.1	121.9	122.3	121.5

The changes (*i.e.*, increases or decreases) on metallation in the bond lengths and bond angles, for each spin state of Fe(II), depend on the type of the bond or angle considered. For instance, the bond lengths (Å) of C4-C5, N6-C7, C9-N12, C13-C17, N18-C19 and C21-N24 bonds decreases by 0.008-0.0116 for s = 0 and increases by 0.005-0.012 for s = 1 and 0.004-0.009 for s = 2. The bond lengths (Å) of N1-C2, N1-C5, C13-N14 and N14-C15 bonds (*i.e.*, the bond on the pyrrole ring on which there are protons on the free Pz) increases by 0.012 for s = 0, ≈0.005 for s = 1 and ≈0.022 for s = 2 while the bond length of C7-N8, N8-C9, C19-N20 and N20-C21 bonds (*i.e.*, bond on the pyrrole rings that are non-protonated in the free Pz) increase by ≈0.014 Å for s = 0 and ≈0.031 Å for s = 2. For s = 1,the C7-N8, N8-C9 increases by 0.011Å while C19-N20 and N20-C21 decreases by 0.017Å. The lengths of the C10-C11 and C22-C23 bonds decreases by 0.001 Å for s = 0, ≈0.010 for s = 1 and increases by 0.034 Å for s = 2. Overall, the results suggest that there are greater geometric changes on the pyrrole rings that are initially non-protonated than on the pyrrole rings that are initially protonated.

The change (*i.e.*, increases or decreases) in the bond angles also depends on the type of the angle considered. The C2N1C5 and C13N14C15 bond angles (*i.e.*, the bond angles on the prole rings that are protonated in the free porphyrazine base) decreases by 4.7º for s = 0, 4.2 for s=1 and 4.5º for s = 2 on metallation while the C7N8C9 and C19N20C21 angles (*i.e.*, the bond angles on the pyrrole rings that are non-protonated in the free porphyrazine base) decreases by 1.2º for s = 0 1 and 1.6º for s = 2 and increases by 1.2º for s = 1. The C2N6C7, C9N12C13, C15N18C19 and C21N24C5 angles increases by 0.5º for s = 0 and s = 2 and decreases by 0.8º for s = 1.

The Mulliken atomic charges of the core porphyrazine fragment for the three compounds are comparatively listed in Table-2 and show that they are affected by both the alkylation and the metallation of the porphyrazine moiety. A comparison of the Mulliken atomic charges on the atoms of the non-alkylated free porphyrazine and the corresponding atoms on the free oct(pr)Pz suggests that the charge on all the atoms become more negative on alkylation, which may be the result of the fact that alkylation has an effect of electron donating towards the pyrrole rings. A comparison of free oct(pr)Pz base and oct(pr)PzFe(II), with iron in different spin states, suggests that the atoms with the most significant increase in the Mulliken atomic charge are N1 and N14 (with an increases of -0.041e for s = 0, 0.008 for s = 1 and -0.084e for s = 2) and N8 and N20 (with an increases of -0.052e for s = 0, -0.075e for s = 1 and -0.133e for s = 2). The meso-bridging atoms N6, N12, N18 and N24 show the least influence by metallation, suggesting that the atoms whose Mulliken atomic charge changes most are those directly bonding to the Fe metal or in the vicinity of the N-Fe bonds.

The electronic transition of porphyrazines is often studied by considering their frontier molecular orbitals (*i.e.*, the highest occupied molecular orbital (HOMO) and the lowest unoccupied molecular orbital (LUMO)) and the corresponding energies, *i.e.*, E_{HOMO}, E_{LUMO} and ΔE, where ΔE is the energy difference between E_{HOMO} and E_{LUMO}. E_{HOMO} describes the electron donating ability of a given molecule, E_{LUMO} describes the electron accepting ability of a molecule and ΔE describes the reactivity tendency of a given molecule[37-42]. The highest occupied molecular orbital for all the compounds considered

are shown in Fig. 3 while the E_{HOMO}, E_{LUMO} and ΔE values, are reported in Table-3. The results suggest that alkylation of the porphyrazine increase the electron donating ability and the reactivity tendency (measured by ΔE gap) and decrease the electron accepting ability of the moiety. The results also show that metallation induces an increase in the electron donating, electron accepting and reactivity tendency of porphyrazine. The increase in the E_{HOMO}, E_{LUMO} and ΔE is dependent on the spin state of Fe(II). Alkylation and metallation also has an effect of increasing the dipole moment of the porphyrazine base.

TABLE-2
MULLIKEN ATOMIC CHARGES ON THE ATOMS OF INTEREST FOR THE STUDIED PORPHYRAZINE DERIVATIVES

Atom	H_2Pz	oct(pr)Pz	oct(pr)PzFe(II) Fe(s=0)	oct(pr)PzFe(II) Fe(s=1)	oct(pr)PzFe(II) Fe(s=2)
N1	-0.705	-0.731	-0.772	-0.739	-0.815
C2	0.523	0.505	0.495	0.496	0.503
N6	-0.553	-0.572	-0.571	-0.572	-0.575
C7	0.485	0.462	0.485	0.494	0.467
N8	-0.639	-0.664	-0.716	-0.739	-0.796
C9	0.484	0.461	0.484	0.495	0.468
N12	-0.553	-0.572	-0.570	-0.572	-0.575
C13	0.524	0.505	0.493	0.494	0.503
N14	-0.705	-0.731	-0.772	-0.739	-0.815
C15	0.523	0.505	0.496	0.495	0.504
N18	-0.553	-0.572	-0.570	-0.572	-0.576
C19	0.485	0.462	0.484	0.495	0.468
N20	-0.639	-0.663	-0.715	-0.739	-0.796
C21	0.484	0.462	0.485	0.495	0.468
N24	-0.553	-0.572	-0.571	-0.572	-0.576

TABLE-3
THE ENERGY (EV) OF THE HOMO, THE LUMO AND ΔE AND THE DIPOLE MOMENT (DEBYE) FOR THE STUDIED DERIVATIVES OF PORPHYRAZINE

Quantum chemical parameter	H_2Pz	oct(pr)Pz	oct(pr)PzFe(II) Fe(s=0)	oct(pr)PzFe(II) Fe(s=1)	oct(pr)PzFe(II) Fe(s=2)
E_{HOMO}	-5.82	-5.30	-5.03	-5.33	-3.87
E_{LUMO}	-3.19	-2.76	-3.06	-2.63	-2.57
ΔE	2.63	2.54	1.97	2.70	1.30
Dipole moment	0.00	0.65	0.72	0.70	0.67

Comparison of the experimental and theoretical data on UV-visible absorption spectra: Ultraviolet and visible absorption spectra provide valuable information on porphyrazine and its derivatives. For instance, UV-visible absorption spectra is reported to determine the therapeutic depth of the treatment in PDT[43]. The values of the Q-band and B-band (both bands attributed to allowed π-π* transition[13]) for the studied porphyrazine derivatives are shown in Table-4. All the compounds show the split Q band with all the experimental and theoretical results and accordingly all the compounds studied have the D2h symmetry[44]. Experimental studies show that the Q band in oct(pr)Pz free base has significant peaks at 626.1 nm and 558.0 nm which equal to a splitting of 68.1 nm. The TDDFT method predicts two Q band peaks at 538.5 nm and 508.6 nm which equal to a splitting of 29.9 nm. Experimental studies show that the Q band in oct(pr)PzFe(II) has a peak at 625.1 nm and at 557.9 nm, corresponding to a splitting of 67.2 nm. The TDDFT method predicts two Q band peaks at 696.0 nm and 545.7 nm, corresponding to a splitting of 150.3 nm for Fe(II) with spin state, s = 0; two Q band peaks at 696.0 nm and 545.7 nm, corresponding to a splitting of 150.3 nm for Fe(II) with spin state, s = 1 and one Q band peak at 952.3 nm for Fe(II) with spin state, s = 2.

The B band (also known as soret band) is reported at 340 nm for experimental results and 364.5 nm for TDDFT results and is only possible for the metal free oct(pr)Pz. TDDFT, also predicts a shoulder band at 443.81 nm for the metal free oct(pr)Pz, which could be attributed to the n→π* transition of the nonbonding electrons on the meso-nitrogen atoms of the macrocycle.

Conclusion

Oct(pr)PzMg(II) was synthesized, demetallated under acid medium to produce oct(pr)Pz base. Iron(II) was incorporated into the oct(pr)Pz base to produce oct(pr)PzFe(II). The compounds were characterized by IR and UV-visible spectroscopy. The results shows that mechanism of incorporation proposed involves a rapid loss of the magnesium ion followed by a slow insertion of the iron(II) cation. The oxidation of the oct(pr)PzFe(II) complex was achieved using the oct(pr)PzCr(II) (III) complex. The redox mechanism proposed

TABLE-4
CALCULATED AND EXPERIMENTAL ABSORPTION PARAMETERS OF H2Pz, oct(pr)Pz AND THEIR oct(pr)PzFe(II) COMPLEXES. PARAMETERS WHICH HAVE OSCILLATOR STRENGTH LESS THAN 0.01 ARE EXCLUDED. THE EXPERIMENTAL ABSORBANCE MEASUREMENTS WERE PERFORMED IN DIMETHYLFORMAMIDE SOLUTION (DMF)

Structure	Calculated absorption parameters			Experimental absorption parameters	
	Wavelength nm	Oscillator strength	Excitation energy (eV)	Wavelength	Absorbance
H_2Pz	521.40	0.1229	2.3779		
	492.00	0.1248	2.5200		
	395.14	0.0994	3.1377		
	384.15	0.0345	3.2275		
oct(pr)Pz	538.47	0.2031	2.3025	626.1	1.244
	508.61	0.1994	2.4377	598.0	0.234
	443.81	0.0344	2.7936	558.0	0.783
	433.56	0.0057	2.8597		
	364.47	0.0946	3.4018	340.0	1.363
oct(pr)PzFe(II), s=0	696.00	0.0704	1.7814	625.1	0.156
	545.67	0.0662	2.2722	557.9	0.121
oct(pr)PzFe(II), s=2	952.28	0.0148	1.3020	625.1	0.156
	948.44	0.0080	1.3072	557.9	0.121

was an outer-sphere electron tunnelling sphere mechanism. Kinetic studies of metallation of the porphyrazines and oxidation of compounds assisted in proposition of the mechanism of metallation. Quantum chemical studies have shown that alkylation affects only electronic parameters (*e.g.*, dipole moment and Mulliken atomic charges) and have no small influences on the geometric properties of the porphyrazine free base. Metallation affects both geometric properties and electronic properties of porphyrazine and the influence is dependent on the spin state of Fe(II).

ACKNOWLEDGEMENTS

Thanks to B. D. G. Williams for the use of his laboratory in the synthesis of the porphyrazine ligand.

REFERENCES

1. E.J. Baerends, G. Ricciardi, A. Rosa and S.J.A. van Gisbergen, *Coord. Chem. Rev.*, **230**, 5 (2002).
2. E.G. Sakellariou, A.G. Montalban, H.G. Meunier, R.B. Ostler, G. Rumbles, A.G.M. Barrett and B.M. Hoffman, *J. Photochem. Photobiol. A-Chem.*, **136**, 185 (2000).
3. H. Ali and J.E. van Lier, *Chem. Rev.*, **99**, 2379 (1999).
4. J.-M. Lehn, Supramolecular Chemistry: Concepts and Perspectives, VCH, Weinheim (1995).
5. G. De la Torre, P. Vazquez, F. Agullo-Lopez and T. Torres, *J. Mater. Chem.*, **8**, 1671 (1998).
6. Z.-C. Sun, Y.-B. She, Y. Zhou, X.-F. Song and K. Li, *Molecules*, **16**, 2960 (2011).
7. J. Haber, L. Matachowski, K. Pamin and J. Poltowicz, *J. Mol. Catal. A: Chem.*, **198**, 215 (2003).
8. O. Zakharieva, A.X. Trautwein and C. Veeger, *Biophys. Chem.*, **88**, 11 (2000).
9. L. Bourre, G. Simonneaux, Y. Ferrand, S. Thibaut, Y. Lajat and T. Patrice, *J. Photochem. Photobiol. B*, **69**, 179 (2003).
10. M. Biesaga, J. Orska, D. Fiertek, J. Izdebski and M. Trojanowicz, *Fresenius J. Anal. Chem.*, **364**, 160 (1999).
11. C.M. Drain, K.C. Russell and J.M. Lehn, *Chem. Commun.*, **3**, 337 (1996).
12. G. Ergün, *J. Chem. Res.*, **2008**, 465 (2008).
13. H. Akkus and A. Gül, *Transition Metal Chem.*, **26**, 689 (2001).
14. J. Tang, L. Chen, J. Sun, K. Lv and K. Deng, *Inorg. Chem. Commun.*, **13**, 236 (2010).
15. X. Zhang, Y. Zhang and J. Jiang, *J. Mol. Struct.*, **673**, 103 (2004).
16. X. Zhang and J. Jiang, *J. Elect. Spectrosc. Rel. Phenom.,* **142**, 145 (2005).
17. X. Zhang, N. Kobayashi and J. Jiang, *Spectrochim. Acta A,* **64**, 526 (2006).
18. Z. Liu, X. Zhang, Y. Zhang, R. Li and J. Jiang, *Spectrochim. Acta A,* **65**, 467 (2006).
19. V.N. Nemykin, R.G. Hadt, R.V. Belosludov, H. Mizuseki and Y. Kawazoe, *J. Phys. Chem. A*, **111**, 12901 (2007).
20. A. Baccouche, B. Peigne´, F. Ibersiene, D. Hammoute`ne, A. Boutarfaia, A. Boucekkine, C. Feuvrie, O. Maury, I. Ledoux and H. LeBozec, *J. Phys. Chem. A*, **114**, 5429 (2010).
21. D. Qi and J. Jiang, *J. Phys. Chem. A*, **115**, 13811 (2011).
22. K.A. Nguyen and R. Pachter, *J. Chem. Phys.*, **114**, 10757 (2001).
23. J. Mack, Y. Asano, N. Kobayashi and M.J. Stillman, *J. Am. Chem. Soc.*, **127**, 17697 (2005).
24. J. Fan, M. Seth, J. Autschbach and T. Ziegler, *Inorg. Chem.*, **47**, 11656 (2008).
25. J. Autschbach, T. Ziegler, S.J.A. van Gisbergen and E.J. Baerends, *J. Chem. Phys.*, **116**, 6930 (2002).
26. Y. Shao, L.F. Molnar, Y. Jung, J. Kussmann, C. Ochsenfeld, S.T. Brown, A.T.B. Gilbert, L.V. Slipehenko, S.V. Levehenko, D.P. O'Neill, R.A. DiStasio Jr., R.C. Lochan, T. Wang, G.J.O. Beran, N.A. Besley, J.M. Herbert, C.Y. Lin, T. Van Voorhis, S.H. Chien, A. Sodt, R.P. Steele, V.A. Rassolov, P.E. Maslen, P.P. Korambath, R.D. Adamson, B. Austin, J. Baker, E.F.C. Byrd, H. Dachsel, R.J. Doerksen, A. Dreuw, B.D. Dunietz, A.D. Dutoi, T.R. Furlani, S.R. Gwaltney, A. Heyden, S. Hirata, C.P. Hsu, G. Kedziora, R.Z. Khalliulin, P. Klunzinger, A.M. Lee, M.S. Lee, W.Z. Liang, I. Lotan, N. Nair, B. Peters, E.I. Proynov, P.A. Pieniazek, Y.M. Rhee, J. Ritchie, E. Rosta, C.D. Sherrill, A.C. Simmonett, J.E. Subotnik, H.L. Woodcock III, W. Zhang, A.T. Bell, A.K. Chakraborty, D.M. Chipman, F.J. Keil, A. Warshel, W.J. Hehre, H.F. Schaefer, J. Kong, A.I. Krylov, P.M.W. Gill and M. Head-Gordon, *Phys. Chem. Chem. Phys.*, **8**, 3172 (2010).
27. M.J. Frisch, G.W. Trucks, H.B. Schlegel, G.E. Scuseria, M.A. Robb, J.R. Cheeseman, J.A. Montgomery, T. Vreven, K.N. Kudin, J.C. Burant, J.M. Millam, S.S. Iyengar, J. Tomasi, V. Barone, B. Mennucci, M. Cossi, G. Scalmani, N. Rega, G.A. Petersson, H. Nakatsuji, M. Hada, M. Ehara, K. Toyota, R. Fukuda, J. Hasegawa, M. Ishida, T. Nakajima, Y. Honda, O. Kitao, H. Nakai, M. Klene, X. Li, J.E. Knox, H.P. Hratchian, J.B. Cross, C. Adamo, J. Jaramillo, R. Gomperts, R.E. Stratmann, O. Yazyev, A.J. Austin, R. Cammi, C. Pomelli, J.W. Ochterski, P.Y. Ayala, K. Morokuma, G.A. Voth, P. Salvador, J.J. Dannenberg, V.G. Zakrzewski, S. Dapprich, A.D. Daniels, M.C. Strain, O. Farkas, D.K. Malick, A.D. Rabuck, K. Raghavachari, J.B. Foresman, J.V. Ortiz, Q. Cui, A.G. Baboul, S. Clifford, J. Cioslowski, B.B. Stefanov, G. Liu, A. Liashenko, P. Piskorz, I. Komaromi, R.L. Martin, D.J. Fox, T. Keith, M.A. Al-Laham, C.Y. Peng, A. Nanayakkara, M. Challacombe, P.M.W. Gill, B. Johnson, W. Chen, M.W. Wong, C. Gonzalez and J.A. Pople, GAUSSIAN 03, Gaussian, Inc., Pittsburgh, PA (2003).
28. R.P. Linstead and M. Whalley, *J. Chem. Soc.*, 4839 (1952).
29. J. Fitzgerald, B.S. Haggerty, A.N. Rheingold and L. May, *Inorg. Chem.*, **31**, 2006 (1992).
30. J. Fitzgerald, W. Taylor and H. Owen, *Synthesis*, 686 (1991).
31. S.J. Lange, H. Nie, C.L. Stern, A.G.M. Barrett and B. Hoffmann, *Inorg. Chem.*, **37**, 6435 (1998).
32. T.P. Forsyth, A.G. Montalban, A.G.M. Barrett and B. Hoffmann, *J. Org. Chem.*, **63**, 331 (1998).
33. B. Cosimelli, G. Roncucci, D. Dei, L. Fantetti, F. Ferroni, M. Ricci and D. Spinelli, *Tetrahedron*, **59**, 10025 (2003).
34. P. Kubát and J. Mosinger, *J. Photochem. Photobiol. A*, **96**, 93 (1996).
35. D.P. Goldberg, A.G. Montalban, A.J.P. White, D.J. Williams, A.G.M. Barrett and B. Hoffmann, *Inorg. Chem.*, **37**, 2873 (1998).
36. M. Gouterman, *J. Chem. Phys.*, **30**, 1139 (1959).
37. B.A. Hess, Jr. and L.J. Schaad, *J. Am. Chem. Soc.*, **93**, 2413 (1971).
38. R.C. Haddon and T. Fukunaga, *Tetrahedron Lett.*, **21**, 1191 (1980).
39. R.G. Pearson, *Proc. Natl. Acad. Sci. USA*, **83**, 8440 (1986).
40. R.G. Pearson, *J. Am. Chem. Soc.*, **110**, 2092 (1988).
41. R.G. Pearson, *J. Org. Chem.*, **54**, 1423 (1989).
42. Z. Zhou, R.G. Parr and J.F. Garst, *Tetrahedron. Lett.*, **29**, 4843 (1988).
43. P. Zimcik, V. Novakova, M. Miletin and K. Kopecky, *Macroheterocycles*, **1**, 21 (2008).
44. N. Kobayashi and H. Konami, in eds.: C.C. Leznoff and A.B.P. Lever, Molecular Orbitals and Electronic Spectra of Phthalocyanine Analogues, in Phthalocyanines: Properties and Applications, VCH Publishers, New York, vol. 4 (1996).